Regular article

A valence-bond-based complete-active-space self-consistent-field method for the evaluation of bonding in organic molecules

Lluís Blancafort[1], Paolo Celani[2,3], Michael J. Bearpark[2], Michael A. Robb[2]

[1] Institut de Química Computacional, Departament de Química, Universitat de Girona, Campus de Montilivi, 17071 Girona, Spain
[2] Department of Chemistry, King's College London, Strand, London, WC2R 2LS, UK
[3] Institut für Theoretische Chemie, Universität Stuttgart, Pfaffenwaldring 55, 70569 Stuttgart, Germany

Abstract. We present the complete-active-space self-consistent-field (CASSCF) implementation of a valence-bond (VB) based method for the analysis of bonding in organic molecules. The method uses the spin-exchange density matrix **P** with a localized orbital basis, where the determinants of the CASSCF wavefunction become VB-like determinants with different spin coupling patterns. The index P_{ij} evaluates the contributions of the determinants to the CASSCF wavefunction and is used to generate resonance formulas. We use the bonding contributions in the original VB formulation of the method ($\alpha\beta$ terms). The method is applied in studies of excited-state reactivity, as shown here for indole. Its first excited state is covalent and is characterized by a decrease in the bond orders in the benzene moiety, similar to the B_{2u} excited state of benzene. In contrast, the ionic excited state has an inversion in the bonds of the pyrrole moiety induced by charge transfer to the benzene ring.

Introduction

One of the classic problems of quantum chemistry is how to characterize the calculated wavefunctions and interpret them in terms of intuitive concepts. To mention a few examples, general bonding-analysis methods can be derived from the electronic density (like methods based on the theory of atoms in molecules) [1] or from an orbital picture (like natural bond order analysis) [2]. Ideas from natural bond order analysis have been recently extended to treat photochemical reactivity [3]. Bond orders for

complete-active-space self-consistent-field (CASSCF) wavefunctions have been calculated from the one-electron reduced density matrix [4]. Related methods for spin-coupled wave-functions use the two-electron reduced density matrix or the weights of the spin functions for the bonding analysis [5, 6]. A different approach evaluates aromaticity using the nucleus-independent chemical shielding [7], in what can be thought of as an indirect bonding measure. In this paper we present the CASSCF implementation of a method based on classic valence bond (VB) theory [8] that calculates the spin-exchange density matrix **P** (which is in turn related to the two-electron reduced density matrix of the CASSCF wavefunction, see Appendix) and gives a quantitative analysis of bonding in molecules. The result can then be expressed in terms of traditional resonance structures.

In previous work, we have applied this method for the analysis of spin multiplicity (singlet versus triplet) [9] and π-type bonding in organic molecules [10, 11, 12, 13]. In particular, our examples have shown that the excited-state reactivity in photochemical problems can be rationalized by the different bond patterns of the electronic states involved. The value of the method is shown here for indole, the chromophore of the aminoacid tryptophan [14]. Indole is a typical organic molecule where the interpretation of the excited states in terms of excitations between molecular orbitals is difficult, because the molecular orbitals are delocalized and the excited states are linear combinations of individual excitations. Platt's notation [15], which was developed for the excited states of hydrocarbons, is useful to characterize the lowest excited states of indole as covalent (^1L_b) and ionic (^1L_a); however, this is insufficient to rationalize its excited-state characteristics, such as the excited-state geometries and the proton-induced fluorescence quenching in tryptophan [12]. This goal is achieved through our method of analysis by using resonance structures to characterize the states.

In what follows we describe the CASSCF implementation and introduce some basic examples in order

Correspondence to: L. Blancafort
e-mail: lluisb@stark.udg.es

to provide the foundations of our analysis. The spin-exchange density matrix evaluates the contribution of VB-like determinants with different spin patterns to a CASSCF wavefunction. One important theoretical point is that the matrix elements P_{ij}, as defined originally in VB theory, are composed of a bonding contribution (pairs of $\alpha\beta$ electrons) and a nonbonding or antibonding one (pairs of $\alpha\alpha$ electrons). The bonding contribution $P_{ij}^{\alpha\beta}$ is the index used in our structural analysis.

General approach and basic examples

The method uses the spin-exchange density matrix P_{ij}. The spin-exchange operator, which interchanges the spin variables 1 and 2, appears in the Dirac identity [16, 17]:

$$[\mathbf{S}(1)\mathbf{S}(2)]\Theta(1,2) = \left(\frac{1}{2}\mathbf{P}_{12} - \frac{1}{4}\mathbf{1}\right)\Theta(1,2),$$

i.e.

$$\mathbf{P}_{12} = \left\langle 2[\mathbf{S}(1)\mathbf{S}(2)] + \frac{1}{2}\mathbf{1} \right\rangle. \tag{1}$$

For a given pair of electrons, the value of the two-electron spin operator $\mathbf{S}(1)\mathbf{S}(2)$ is $-3/4$ for paired spins, 0 for uncoupled spins and $1/4$ for parallel spins [17]. In our analysis we use the negative value of the elements of the orbital representation, P_{ij}. Using Eq. (1), they become $+1$, $-1/2$ and -1 for pairs of paired, uncoupled and parallel spins, respectively. For wavefunctions composed of several VB structures "in resonance", the values of P_{ij} give a quantitative measure of the bonding, as suggested early by Penney and Moffitt [18]. Further, the trace of $\mathbf{P}$ is related to the total spin by [16]

$$S(S+1) = -\frac{1}{4}[N(N-4)] + \sum_{ij} P_{ij}.$$

For the CASSCF implementation, the delocalized orbitals of the active space are localized on the atoms (i.e. the active space must be big enough to give a good localization). In that case, the CASSCF wavefunction becomes equivalent to an "extended" VB one. It contains the "covalent" determinants (where every localized orbital is occupied by one electron) of a VB function and additional "ionic" determinants (with some orbitals occupied by two or zero electrons). In our examples, the active space of the CASSCF calculation consists mainly of π orbitals, and the calculated P_{ij} elements generally give the π bonding between two sites i and j. However, the method is also applicable to σ bonding, including σ orbitals in the active space (see the examples of σ-bond forming reactions later). Most of the examples given later are covalent hydrocarbons where the overall occupation of the localized orbitals is of one electron. Nevertheless, one of our examples for excited states (^1L_a state of indole, see later) has significant charge-transfer

character. In that case it is useful to examine also the diagonal elements of the one-electron matrix (D_{ii}), which give the orbital occupations.

The most significant result from the derivation of an expression for the spin-exchange density matrix $\mathbf{P}$ (see Appendix) is that the final value of the P_{ij} elements is the difference between $\alpha\beta$ and $\alpha\alpha$ terms:

$$P_{ij} = P_{ij}^{\alpha\beta} - P_{ij}^{\alpha\alpha}, \tag{2}$$

where the terms for spin-adapted Hartree–Waller determinants [19] are given by

$$P_{ij}^{\alpha\beta} = \frac{1}{2}\sum_{K,L} c_K c_L \langle \phi_K | a_{i\alpha}^+ a_{j\alpha} a_{j\beta}^+ a_{i\beta} | \phi_L \rangle \tag{3a}$$

and

$$P_{ij}^{\alpha\alpha} = \frac{1}{2}\sum_{K} c_K^2 \langle \phi_K | a_{i\alpha}^+ a_{j\alpha}^+ a_{j\alpha} a_{i\alpha} | \phi_K \rangle. \tag{3b}$$

The $\alpha\beta$ and $\alpha\alpha$ terms that appear in the general formula of Eq. (2) represent the bonding and the nonbonding or antibonding contributions to the spin-exchange density, respectively. The bonding contribution comes from the positive $\alpha\beta$ terms where electrons i and j have opposite spin (i.e. singlet coupling). In contrast to this, the nonbonding or antibonding $\alpha\alpha$ terms arise from configurations where the two electrons have the same spin (i.e. uncoupled or triplet coupling) and give a negative contribution. The calculation of the $\alpha\alpha$ terms is straightforward, because they are composed of the squared coefficients of configurations Φ_K that have i and j electrons of the same spin. On the other hand, the $\alpha\beta$ contributions are generated by two determinants Φ_K and Φ_L that differ only in the relative spin of two electrons (Fig. 1). The calculation of these terms is shown later for two simple examples. We will focus on the behavior of the bonding component $P_{ij}^{\alpha\beta}$, which is the index used in our CASSCF-based analysis of ground-state and excited-state structures. We finally note that our analysis only considers interactions between neighboring atoms. Atoms viz. orbitals that lie far apart (for example meta and para positions in benzene) also give nonzero $P_{ij}^{\alpha\beta}$ components. However, the VB energy expression [8] where the P_{ij} terms appear, is
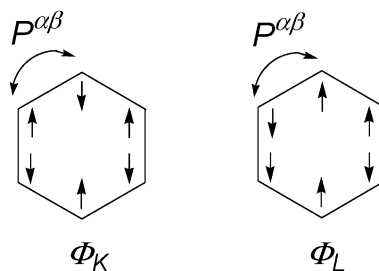

Fig. 1. Example of two benzene configuration-state functions coupled by the $\alpha\beta$ term of the P_{ij} operator
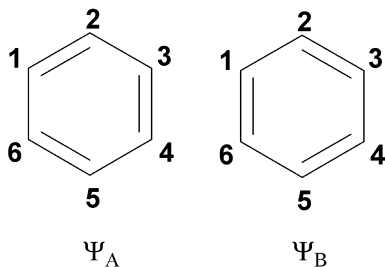
Fig. 2. Kekulé forms for benzene

$$E = Q + \sum_{ij} P_{ij} K_{ij}.$$

For nonneighboring atom pairs, the exchange integral K_{ij} tends to zero, and these terms have no effect on the energy. They are therefore not considered in our analysis.

Spin-exchange elements for and ideal VB function of benzene

We start our discussion of the P_{ij} bond indices with the calculation of P_{ij} values for an idealized wavefunction of benzene made only of Kekulé-type configurations, where the small number of configurations allows the P_{ij} elements to be derived "by hand". To facilitate the comparison with the CASSCF results, the wavefunction is expressed with spin-adapted Hartree–Waller configurations rather than with the traditional spin functions of VB theory (e.g. Rumer functions). For one of the Kekulé structures (Ψ_A, Fig. 2), the four spin-adapted configurations that describe this structure are (upper rows refer to orbitals occupied by α electrons and lower rows to orbitals occupied by β electrons)

$$\Phi_1 = \begin{vmatrix} 2 & 4 & 6 \\ 1 & 3 & 5 \end{vmatrix}\Bigg\rangle, \; \Phi_2 = \begin{vmatrix} 2 & 4 & 5 \\ 1 & 3 & 6 \end{vmatrix}\Bigg\rangle, \; \Phi_3 = \begin{vmatrix} 2 & 3 & 6 \\ 1 & 4 & 5 \end{vmatrix}\Bigg\rangle,$$

$$\Phi_4 = \begin{vmatrix} 2 & 3 & 5 \\ 1 & 4 & 6 \end{vmatrix}\Bigg\rangle.$$

The VB wavefunction corresponding to the pure resonance structure is

$$\Psi_A = \frac{1}{2}(\Phi_1 + \Phi_2 + \Phi_3 + \Phi_4),$$

i.e. normalization factor 0.5 for the four determinants, where we assume that the determinants are orthogonal to each other. For π-bonded neighboring atoms (for example carbon atoms 1 and 2 in Fig. 1), the $\alpha\alpha$ component is 0, and the $\alpha\beta$ one is

$$P_{12}^{\alpha\beta} = (c_1 c_4 + c_2 c_3 + c_3 c_2 + c_4 c_1) = 1.00$$

(for all P_{ij} terms, the factor 0.5 of Eq. 3a is compensated by the fact that the final value is obtained as the sum of two equal terms, P_{ij} and P_{ji}). For the nonbonded neighboring atoms (e.g. carbon atoms 2 and 3 in Fig. 1), the $\alpha\beta$ terms are zero, and the $\alpha\alpha$ ones are

$$P_{23}^{\alpha\alpha} = (c_3^2 + c_4^2) = 0.50.$$

Thus the total spin-exchange values P_{ij} for bonded and nonbonded atoms are 1.00 and −0.50, respectively.

We now consider "resonant" benzene, which is the mixture of the resonance structures Ψ_A and Ψ_B. The determinants for Ψ_B are

$$\Phi_1 = \begin{vmatrix} 2 & 4 & 6 \\ 1 & 3 & 5 \end{vmatrix}\Bigg\rangle, \; \Phi_5 = \begin{vmatrix} 3 & 4 & 6 \\ 1 & 2 & 5 \end{vmatrix}\Bigg\rangle, \; \Phi_6 = \begin{vmatrix} 2 & 5 & 6 \\ 1 & 3 & 4 \end{vmatrix}\Bigg\rangle,$$

$$\Phi_7 = \begin{vmatrix} 3 & 5 & 6 \\ 1 & 2 & 4 \end{vmatrix}\Bigg\rangle.$$

Assuming orthogonality of the determinants, the corresponding wave-function is

$$\Psi_B = \frac{1}{2}(\Phi_1 + \Phi_5 + \Phi_6 + \Phi_7)$$

and the final, normalized "resonant" wave-function is

$$\Psi_{res} = \frac{1}{\sqrt{2}}(\Psi_A + \Psi_B)$$

$$= \frac{1}{\sqrt{10}}(2\Phi_1 + \Phi_2 + \Phi_3 + \Phi_4 + \Phi_5 + \Phi_6 + \Phi_7).$$

The six P_{ij} elements for neighboring atoms are now equivalent, and the components are

$$P_{12}^{\alpha\alpha} = (c_5^2 + c_7^2) = 0.20$$

and

$$P_{12}^{\alpha\beta} = (c_1 c_4 + c_2 c_3 + c_3 c_2 + c_4 c_1) = 0.60.$$

The final value is

$$P_{12} = P_{12}^{\alpha\beta} - P_{12}^{\alpha\alpha} = 0.40.$$

It is clear that the delocalization of the wavefunction leads to the appearance of new nonbonding $\alpha\alpha$ terms and to a decrease of the bonding $\alpha\beta$ terms. Thus, the $\alpha\beta$ term that is the bonding index of our analysis decreases from 1.00 for idealized bezene (single resonance structure) to 0.60 (resonating structures).

Effect of heteroatoms and ionic configurations

The effect of heteroatoms with doubly occupied, localized π orbitals on the calculated P_{ij} values is exemplified for a simple wavefunction of vinylamine (Fig. 3):

$$\Psi_{VA} = \frac{1}{\sqrt{2}}(\Phi_1 + \Phi_2),$$

where the two determinants are

$$\Phi_1 = \left| \begin{matrix} 1 & 2 \\ 1 & 3 \end{matrix} \right\rangle, \ \Phi_2 = \left| \begin{matrix} 1 & 3 \\ 1 & 2 \end{matrix} \right\rangle.$$

For centers 1 and 2 the $\alpha\alpha$ term is

$$P_{12}^{\alpha\alpha} = (c_1^2 + c_2^2) = 1.$$

In contrast to this, the $\alpha\beta$ term is 0, because the configurations that would give $\alpha\beta$ contributions with Φ_1 or Φ_2 would have two electrons of the same spin in the same orbital and would be forbidden. The absence of a bond between N_1 and C_2 is thus clear from the 0 value of the bonding index $P_{ij}^{\alpha\beta}$. The total value of P_{12} is -1. The same applies for "ionic" configurations, where localized π orbitals on carbon atoms are occupied by two electrons.

Computational details

The VB analyses were carried out as single-point CASSCF/6-31G* calculations, using Boys' procedure to localize the orbitals [20]. The geometries of the minima were optimized at the HF/6-31G* level. For the Cope and Diels–Alder transition structures, the geometries were optimized at the CASSCF/6-31G* level, because analyses on the B3LYP/6-31G* optimized geometries [21] (CASSCF single-point calculations) gave significantly different results. The active spaces (number of electrons and orbitals) were (2,2) for ethylene, (4,4) for butadiene, (6,5) for pyrrole, (6,6) for benzene, the Cope and the Diels–Alder transition structures, and (10,9) for indole. The geometries reported for indole were optimized at the CASS-CF(10,9)/6-31G* level. The code to calculate the CASSCF spin-exchange density matrix has been implemented in Gaussian98 (see Appendix for details) [22].

Computational results

Ground-state examples

The spin-exchange elements $P_{ij}^{\alpha\beta}$ for the ground state of several structures (minima and transition states) are shown in Figs. 4 and 5. The general idea is that the deviation of the CASSCF-based values from the ideal one for localized bonds (i.e. $P_{ij}^{\alpha\beta} = 1$ for singlet coupled pairs) comes from delocalization (i.e. resonance of covalent VB structures, as shown for VB benzene), and from determinants with doubly occupied orbitals (i.e. heteroatoms or ionic terms) that are included in the CASSCF function.
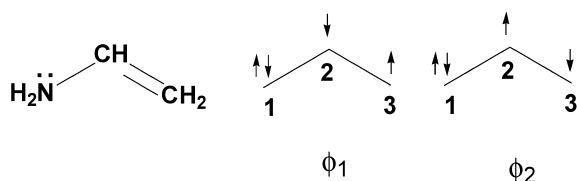
Fig. 3. Configurations for vinylamine

In ethylene (Fig. 4a) and butadiene (Fig. 4b), the $P_{ij}^{\alpha\beta}$ elements for the localized double bonds are smaller than 1 because configuration interaction with ionic structures lowers the coefficients. In the case of butadiene, there are also covalent structures with different bonding patterns that contribute to the decrease of the values to 0.696 and 0.074 for the localized bond and the uncoupled carbons, respectively. For pyrrole (Fig. 4c), we find significant delocalization of the double bonds and some aromatic character. Thus, the $P_{ij}^{\alpha\beta}$ value for the double bond is decreased with respect to ethylene and butadiene. At the same time, the value of the uncoupled carbon–carbon and carbon–nitrogen π bonds is increased with respect to ehylene and vinyl amine, respectively.

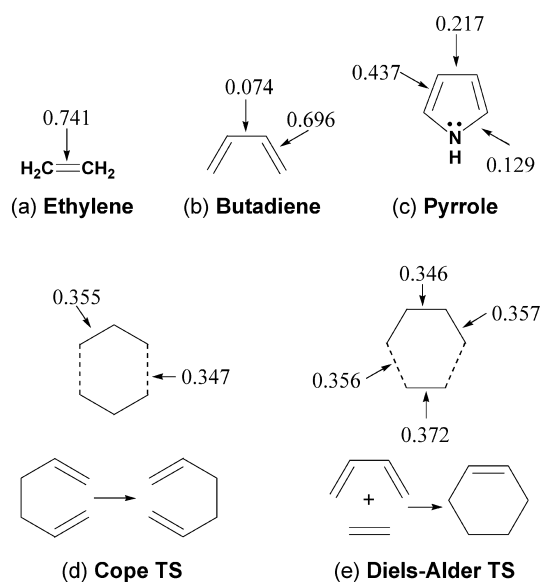These effects are shown in detail for benzene in Fig. 5, which shows the three dominating types of

Fig. 4a–e. Spin-exchange density matrix elements P_{ij} ($\alpha\beta$ terms) for ground-state organic structures (CASSCF/6-31G*)
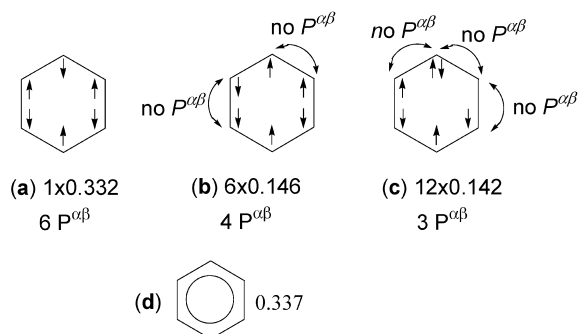
Fig. 5a–d. Dominant configurations (Hartree–Waller determinants) for ground-state benzene, CASSCF(6,6)/6-31G*. d Spin-exchange density matrix elements P_{ij} ($\alpha\beta$ terms), equal for the six C–C bonds

Hartree–Waller determinants and the corresponding coefficients. The main configuration (coefficient 0.332) has alternating α and β spins along the six bonds and contributes to the $P_{ij}^{\alpha\beta}$ elements for the six carbon–carbon π bonds. However, there are six more covalent determinants (coefficient 0.146 each) with parallel spins on neighboring carbon atoms that only contribute to four $P_{ij}^{\alpha\beta}$ elements each. Finally, there are 12 ionic terms (coefficient 0.142 each) that contribute to three $P_{ij}^{\alpha\beta}$ elements each. Overall, this leads to a decrease of the ideal value for $P_{ij}^{\alpha\beta}$ in benzene from 0.6 (VB calculation) to 0.337 for the CASSCF wavefunction.

We also consider the Diels–Alder cycloaddition (ethylene plus butadiene) and the Cope rearrangement for 1,5-hexadiene. Different studies [6, 23] give aromatic character to the transition structures for these reactions, and our VB-type analysis for the CASSCF-optimized transition structures (Fig. 4d, e) agrees with this interpretation. All calculated $P_{ij}^{\alpha\beta}$ values lie around 0.35, which compares well with the value of 0.337 obtained for benzene at the CASSCF level.

Characterization of excited states

Our VB-type analysis is particularly useful to characterize excited states of organic molecules with resonance structures [10, 11, 12, 13]. To get to the final goal of characterizing the excited states using resonance structures, the most convenient starting point is to characterize the ground state. The excited-state resonance structures can then be obtained using the ground state as a reference and examining the most significant changes in the spin-exchange density and in the orbital occupations. The VB structures are helpful to rationalize the optimized geometries for these states, as shown for the intramolecular quenching of the indole chromophore fluorescence in tryptophan [12].

The lowest excited states of indole are a covalent one (S$_1$ at the Franck–Condon geometry, ^{1}L$_b$ in Platt's nomenclature [15]) and an ionic or charge-transfer one (S$_2$, ^{1}L$_a$). In terms of molecular orbital excitations, the ^{1}L$_b$ state at the CASSCF level is composed of two main configurations, the HOMO-1 to LUMO and HOMO to LUMO + 1 excitations, with weights of 44 and 22%, respectively. The ^{1}L$_a$ state is dominated by the HOMO-to-LUMO excitation (54%), and several configurations make for the remaining 46%. Our goal is to simplify the complicated molecular-orbital picture by using our VB-based analysis, which provides a compact bonding index that can be expressed as resonance structures. We note that a quantitative study of the energetics of the excited states requires the inclusion of dynamic correlation (see the CAS-PT2 study of Serrano-Andrés and Roos) [24], but the states can be characterized at the CASSCF level. Because one of the states has significant charge-transfer character, we include in our analysis the diagonal elements of the one-electron matrix (D_{ii}), which give the occupation numbers of the localized

orbitals. For a pure covalent wavefunction, the occupations should be 1.00 on the carbon atoms and 2.00 on the nitrogen orbitals of indole. Occupations significantly different from 1.00 are shown with arrows in Fig. 6.

The ground-state wavefunction at the Franck–Condon geometry is the reference for our excited-state analysis. It has localized double bonds and a doubly occupied nitrogen π orbital (Fig. 6a). This qualitative picture is based on the $P_{ij}^{\alpha\beta}$ values for the neighboring atom pairs C$_2$–C$_3$, C$_4$–C$_5$ and C$_6$–C$_7$, which lie between 0.39 and 0.48, approximately. For the C$_8$–C$_9$ bond, the $P_{ij}^{\alpha\beta}$ value is reduced to 0.26, presumably because of the strain due to ring fusion. The occupation numbers of the localized orbitals support the proposed resonant structure, because the occupation of the nitrogen orbital, 1.70, is close to 2.0. Finally, the resonance structure agrees with the calculated bond lengths, with shorter lengths for the proposed double bonds (1.35–1.38 Å). The C$_8$–C$_9$ double bond is slightly longer for the reason mentioned previously.

Resonance structures for the excited states are obtained by examining the most significant changes in the spin-exchange density and the orbital occupations. According to our analysis, the covalent excitation (^{1}L$_b$, S$_1$) is centered on the benzene moiety of the chromophore (Fig. 6b). Thus, the occupations of the localized orbitals are similar to the ones obtained for the ground-state wavefunction, and the $P_{ij}^{\alpha\beta}$ elements for the N$_1$–C$_2$, C$_2$–C$_3$ and N$_1$–C$_8$ atom pairs virtually do not change. Thus, the covalent excitation does not affect
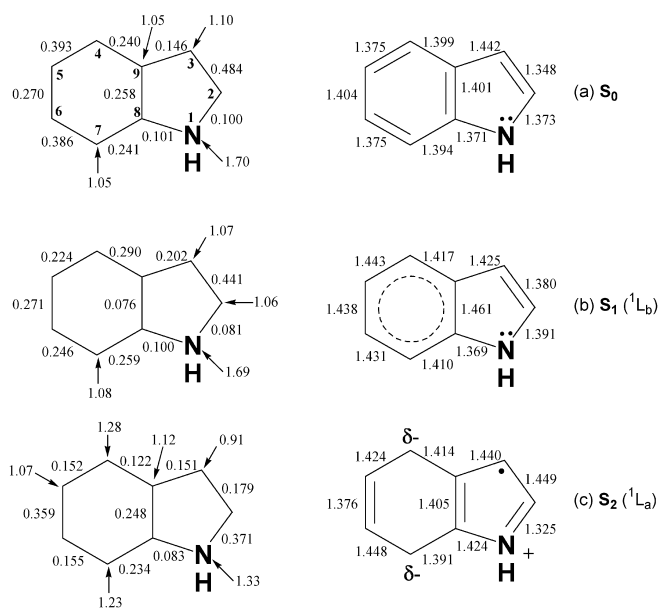

Fig. 6a–c. Spin-exchange density matrix elements P_{ij} ($\alpha\beta$ terms) for the three lowest singlet excited states of indole (*left*), and optimized geometries for the states (*right*), CASSCF(10,9)/6-31G*. The *numbers* shown with *arrows* are the occupation numbers of the localized orbitals (diagonal elements of the one-electron matrix, D_{ii}) that differ significantly from 1.00

the nitrogen π electrons and the pyrrole double bond. In contrast to this, the values for the C_4–C_5, and C_6–C_7 pairs decrease from 0.39 to 0.24, while the one for the C_8–C_9 pair decreases from 0.26 to 0.08 (i.e. the two electrons on these carbon atoms are uncoupled). The decrease of the $P_{ij}^{\alpha\beta}$ elements in the benzene moiety parallels the uncoupling of the π electrons found for the covalent ($^1B_{2u}$) excited state of benzene, where the values for the carbon–carbon bonds decrease from 0.34 in the ground state to 0.25 in the excited state. The general decrease of the π-bond order in the benzene moiety is reflected in the optimized geometry for this state, where the bond lengths increase by up to 0.06 Å, and the proposed resonance structure is shown in Fig. 6b.

For the second excited state, the charge-transfer character is clear from the occupations of the localized orbitals (Fig. 6c). The charge transfer takes place mainly from the nitrogen atom (occupation decreases by 0.37 electrons with respect to the ground state) to the C_4 and C_7 carbons, which take up approximately 0.2 electrons each. This causes a bond inversion in the pyrrole moiety. Thus, a π bond between N_1 and C_2 is formed to stabilize the positive charge on the nitrogen (see the resonance structure), as seen in the increase in the $P_{ij}^{\alpha\beta}$ element from 0.10 to 0.37 and the decrease of the C_2–C_3 value from 0.48 to 0.18. At the same time, the N_1–C_2 and C_2–C_3 bond lengths optimized for this state are inverted with respect to the ground-state geometry. In the benzene moiety, the C_8–C_9 π-bond character is retained and the C_4–C_5 and C_6–C_7 one is lost ($P_{ij}^{\alpha\beta}$ decrease from approximately 0.39 to 0.15) because of the charge transfer to C_4 and C_7. This allows for an increase in the coupling between C_5 and C_6 (increase in $P_{ij}^{\alpha\beta}$ values from 0.27 to 0.36), which leads to a decrease in the corresponding bond length optimized for S_2, from 1.40 to 1.38 Å. Thus, the proposed resonance structure has double bonds between N_1 and C_2, and C_5 and C_6, respectively, and the negative charge is shared between C_4 and C_7. There is also some radical character on C_3, as seen from the small $P_{ij}^{\alpha\beta}$ with neighboring atoms (0.15 and 0.18) and the large distances (1.44 and 1.45 Å). Our calculations on the photochemistry of the amino acid tryptophan [12] show that the ionic excited state is responsible for the proton-transfer-induced quenching of fluorescence observed experimentally. Thus, the transfer of charge density to the C_4 and C_7 positions agrees with the experimental observation of intramolecular excited-state protonation of C_4 in tryptophan [25].

Conclusions

Our VB-based bonding-analysis method characterizes electronic states (ground and excited states from CASSCF calculations) in terms of resonance structures. In the present paper we have shown the foundations of the method together with a few representative examples. Its general value and applicability has been proved in several studies of different excited-state processes, such as double-bond isomerizations [10], energy transfer [11] and proton transfer [12]. The method can also be successfully applied to rationalize the behavior of n,π^* excited states, as shown for the ultrafast radiationless decay of cytosine [13].

The bond-order analysis proposed by Ruedenberg [4] for CASSCF is similar to the VB-based one presented here because it uses localized active orbitals; however, it is based on the one-electron reduced density matrix. Our VB-derived bond indices are part of the two-electron reduced density matrix, and this allows the separation of the bonding ($\alpha\beta$, $\beta\alpha$) from the antibonding ($\alpha\alpha$, $\beta\beta$) components (see Appendix for details). The calculation of bond indices from the two-electron density matrix of a multireference wavefunction was proposed by the groups of Cooper and Ponec [5], using a spin-coupled wave-function. The authors suggested a partition of the two-electron density matrix elements into singletlike and tripletlike components, using a different scheme from the one proposed here. However, the use of a CASSCF function with a localized orbital basis gives greater flexibility since it allows the treatment of ionic states and a more general approach to reactivity. For excited states, a different approach to the one presented here has been proposed by Zimmerman and Alabugin [3], using natural hybrid orbitals. The method analyzes the changes in the electronic density imposed by the electronic excitation in the molecule of interest, at the Franck–Condon geometry. In fact, our experience with the VB-based method presented here is that the use of the ground-state wavefunction as a reference point makes the rationalization of the excited state easier. Therefore, the methodology of Zimmerman and Alabugin can be of complementary value to the one proposed here. However, we note that photochemical and photophysical behavior is often the result of the interaction between several electronic states along a given reaction coordinate [10]. In these cases, for a full mechanistic rationalization it is necessary to study the complete reaction coordinate.

Appendix

Derivation of a second-quantization expression and implementation for CASSCF

It is convenient to express the spin-exchange operator using second quantization, where the general expression for a two-electron operator is [26]:

$$\langle\Psi|\hat{O}_2|\Psi\rangle = \frac{1}{2}\sum_{ijkl}\langle i(1)j(2)|\hat{O}(1,2)|k(1)l(2)\rangle$$
$$\times\langle\Psi|a_i^+a_j^+a_la_k|\Psi\rangle.$$

The corresponding expression for the spin-exchange operator, using Eq. (1), is (from here on we operate with the negative quantity of the original operator)

$$\langle\Psi|\hat{P}_{12}|\Psi\rangle = -\sum_{ijkl}\langle i(1)j(2)|S(1)S(2)+\frac{1}{4}I|k(1)l(2)\rangle$$
$$\times\langle\Psi|a_i^+a_j^+a_la_k|\Psi\rangle.$$

The orbitals are split into spatial terms (indices i,j,k,l) and pure-spin terms (indices μ,η,γ,π), yielding

$$\left\langle 2[\mathbf{S}(1)\mathbf{S}(2)]+\frac{1}{2}\mathbf{1}\right\rangle = -\sum_{\substack{\mu\eta\gamma\pi\\ijkl}}\left(\langle i(1)\mu(1)j(2)\eta(2)|S(1)S(2)+\tfrac{1}{4}I(1)I(2)|k(1)\gamma(1)l(2)\pi(2)\rangle\cdot\langle\Psi|a_{i\mu}^+a_{j\eta}^+a_{l\pi}a_{k\gamma}|\Psi\rangle\right).$$

The spatial integrals are separated and resolved as Kroneker-δ terms δ_{ik} and δ_{jl}, and the spin operator $S(1)S(2)$ is expressed using step-up and step-down operators, such that

$$S(1)S(2) = \frac{1}{2}[S_+(1)S_-(2)+S_-(1)S_+(2)]+S_z(1)S_z(2).$$

Evaluation of the $S(1)S(2)$ part for the different spin combinations over μ,η,γ and π yields

$$\langle 2[\mathbf{S}(1)\mathbf{S}(2)]\rangle = -\sum_{ij}\left(\begin{array}{l}\frac{1}{2}\langle\Psi|a_{i\alpha}^+a_{j\beta}^+a_{j\alpha}a_{i\beta}|\Psi\rangle+\frac{1}{2}\langle\Psi|a_{i\beta}^+a_{j\alpha}^+a_{j\beta}a_{i\alpha}|\Psi\rangle+\frac{1}{4}\langle\Psi|a_{i\alpha}^+a_{j\alpha}^+a_{j\alpha}a_{i\alpha}|\Psi\rangle\\ -\frac{1}{4}\langle\Psi|a_{i\beta}^+a_{j\alpha}^+a_{j\alpha}a_{i\beta}|\Psi\rangle-\frac{1}{4}\langle\Psi|a_{i\alpha}^+a_{j\beta}^+a_{j\beta}a_{i\alpha}|\Psi\rangle+\frac{1}{4}\langle\Psi|a_{i\beta}^+a_{j\beta}^+a_{j\beta}a_{i\beta}|\Psi\rangle\end{array}\right).$$

The part of the identity operator yields

$$\left\langle\frac{1}{2}\mathbf{1}\right\rangle =$$
$$-\sum_{ij}\left(\begin{array}{l}\frac{1}{4}\langle\Psi|a_{i\alpha}^+a_{j\alpha}^+a_{j\alpha}a_{i\alpha}|\Psi\rangle+\frac{1}{4}\langle\Psi|a_{i\beta}^+a_{j\alpha}^+a_{j\alpha}a_{i\beta}|\Psi\rangle\\ +\frac{1}{4}\langle\Psi|a_{i\alpha}^+a_{j\beta}^+a_{j\beta}a_{i\alpha}|\Psi\rangle+\frac{1}{4}\langle\Psi|a_{i\beta}^+a_{j\beta}^+a_{j\beta}a_{i\beta}|\Psi\rangle\end{array}\right).$$

Adding the terms, we obtain the final expression

$$P_{ij} = \frac{1}{2}\langle\Psi|a_{i\alpha}^+a_{j\alpha}a_{j\beta}^+a_{i\beta}+a_{i\beta}^+a_{j\beta}a_{j\alpha}^+a_{i\alpha}-a_{i\alpha}^+a_{j\alpha}^+a_{j\alpha}a_{i\alpha}$$
$$-a_{i\beta}^+a_{j\beta}^+a_{j\beta}a_{i\beta}|\Psi\rangle,$$

where we use the fact that creation and annihilation operators for different spin orbitals are anticommutative. For our purposes, it is convenient to separate the exchange density matrix elements into two terms:

$$P_{ij}^{\alpha\beta} = \frac{1}{2}\langle\Psi|(a_{i\alpha}^+a_{j\alpha}a_{j\beta}^+a_{i\beta}+a_{i\beta}^+a_{j\beta}a_{j\alpha}^+a_{i\alpha})|\Psi\rangle$$

and

$$P_{ij}^{\alpha\alpha} = \frac{1}{2}\langle\Psi|\left(a_{i\alpha}^+a_{j\alpha}^+a_{j\alpha}a_{i\alpha}+a_{i\beta}^+a_{j\beta}^+a_{j\beta}a_{i\beta}\right)|\Psi\rangle,$$

so that

$$P_{ij} = P_{ij}^{\alpha\beta}-P_{ij}^{\alpha\alpha}$$

Thus, the exchange density matrix elements are the difference between exchange terms for electrons of different and same spin, respectively. For a multi-configuration wavefunction expressed in terms of Slater determinants ϕ_K, the elements become

$$P_{ij}^{\alpha\beta} = \frac{1}{2}\sum_{K,L}c_Kc_L\langle\phi_K|(a_{i\alpha}^+a_{j\alpha}a_{j\beta}^+a_{i\beta}+a_{i\beta}^+a_{j\beta}a_{j\alpha}^+a_{i\alpha})|\phi_L\rangle$$
$$= \frac{1}{2}\sum_{K,L}c_Kc_LB_{ij}^{\alpha\beta}.$$

The spin-coupling coefficients $B_{ij}^{\alpha\beta}$ are $+1$ for configurations (i.e. Slater determinants) that differ only in the relative spin of two electrons, and 0 otherwise. For the same-spin terms,

$$P_{ij}^{\alpha\alpha} = \frac{1}{2}\sum_{K,L}c_Kc_L\langle\phi_K|(a_{i\alpha}^+a_{j\alpha}^+a_{j\alpha}a_{i\alpha}+a_{i\beta}^+a_{j\beta}^+a_{j\beta}a_{i\beta})|\phi_L\rangle$$
$$= \frac{1}{2}\sum_{K,L}c_Kc_LB_{ij}^{\alpha\alpha}.$$

Here the coefficients $B_{ij}^{\alpha\alpha}$ are $+1$ for configurations with electrons i,j of the same spin and 0 otherwise.

Relationship to the two-electron reduced density matrix

The general formula for the two-electron reduced density matrix is

$$\Pi(\mathbf{x}_1,\mathbf{x}_2,\mathbf{x}_1',\mathbf{x}_2') = N(N-1)\int d\mathbf{x}_3...d\mathbf{x}_N\Psi(\mathbf{x}_1,\ldots,\mathbf{x}_N)$$
$$\times\Psi^*(\mathbf{x}_1,\ldots,\mathbf{x}_N).$$

For a multireference wavefunction, the two-electron reduced density for the N electrons of the active space is

$$\Pi(\mathbf{x}_1,\mathbf{x}_2,\mathbf{x}_1',\mathbf{x}_2') = N(N-1)\sum_{KL}c_Kc_L^*$$
$$\times\int d\mathbf{x}_3...d\mathbf{x}_N\Phi_K(\mathbf{x}_1,\ldots,\mathbf{x}_N)\times\Phi_L^*(\mathbf{x}_1,\ldots,\mathbf{x}_N).$$

The discrete representation in the basis of the (localized) active orbitals is

$$\Pi_{ijkl} = \int d\mathbf{x}_1d\mathbf{x}_2d\mathbf{x}_1'd\mathbf{x}_2'\chi_i^*(\mathbf{x}_1)\chi_j^*(\mathbf{x}_2)\Pi(\mathbf{x}_1,\mathbf{x}_2,\mathbf{x}_1',\mathbf{x}_2')$$
$$\chi_k(\mathbf{x}_1')\chi_l(\mathbf{x}_2') = \sum_{KL}c_Kc_L\sum_{\mu\nu}\langle\Phi_K|a_{i\mu}^+a_{j\nu}^+a_{k\mu}a_{l\nu}|\Phi_L\rangle,$$

where χ_i are spin orbitals, μ and v are spin variables and the coefficients c are assumed to be real [27]. Our P_{ij} indices (spin-exchange density matrix elements) correspond to the bidiagonal terms Π_{ijji}, i.e.

$$
\Pi_{ijji} = \sum_{KL} c_K c_L
$$
$$
\times \left(\begin{array}{c} \langle \Phi_K | a_{i\alpha}^+ a_{j\alpha}^+ a_{k\alpha} a_{l\alpha} | \Phi_L \rangle + \langle \Phi_K | a_{i\alpha}^+ a_{j\beta}^+ a_{k\alpha} a_{l\beta} | \Phi_L \rangle \\ + \langle \Phi_K | a_{i\beta}^+ a_{j\alpha}^+ a_{k\beta} a_{l\alpha} | \Phi_L \rangle + \langle \Phi_K | a_{i\beta}^+ a_{j\beta}^+ a_{k\beta} a_{l\beta} | \Phi_L \rangle \end{array} \right).
$$

The corresponding formula for the one-electron reduced density matrix indices [4] (P_{ij}^{le}) is

$$
P_{ij}^{le} = \sum_{KL} c_K c_L \sum_{\mu} \langle \Phi_K | a_{i\mu}^+ a_{j\mu} | \Phi_L \rangle.
$$

In contrast to the spin-exchange density matrix elements, these one-electron terms are zero for the benzene VB example just described.

Implementation

For the spin-exchange density matrix elements, the spin-coupling coefficients B_{ij} are calculated on the fly, using the method of direct reduced lists implemented recently for configuration-interaction -vector evaluation [28]. In practice, the matrix **P** is diagonal (i.e. $P_{ij} = P_{ji}$), and the bond order between two centers i and j is obtained by calculating the element once and multiplying by 2. When spin-adapted Hartree–Waller determinants are used instead of Slater ones, the equations given previously are simplified and we obtain

$$
P_{ij}^{\alpha\beta} = \frac{1}{2} \sum_{K,L} c_K c_L \langle \phi_K | a_{i\alpha}^+ a_{j\alpha} a_{j\beta}^+ a_{i\beta} | \phi_L \rangle
$$

and

$$
P_{ij}^{\alpha\alpha} = \frac{1}{2} \sum_{K,L} c_K c_L \langle \phi_K | a_{i\alpha}^+ a_{j\alpha}^+ a_{j\alpha} a_{i\alpha} | \phi_L \rangle
$$
$$
= \frac{1}{2} \sum_{K,L} c_K^2 \langle \phi_K | a_{i\alpha}^+ a_{j\alpha}^+ a_{j\alpha} a_{i\alpha} | \phi_K \rangle.
$$

For the $\alpha\alpha$ terms, a further simplification is given by the fact that ϕ_K and ϕ_L must be the same configuration.

The code for calculation of the spin-exchange density matrix is available in Gaussian98 [22].

References

1. Bader RFW (1994) Atoms in molecules—a quantum theory. Clarendon, Oxford
2. Reed A, Curtiss LA, Weinhold F (1988) Chem Rev 88:899–926
3. Zimmerman HE, Alabugin IV (2000) J Am Chem Soc 122:952–953
4. (a) Feller DF, Schmidt MW, Ruedenberg K (1982) J Am Chem Soc 104:960–967; (b) Schmidt MW, Gordon MS (1998) Annu Rev Phys Chem 49:233–266
5. Cooper DL, Ponec R, Thorsteinsson T, Rao G (1996) Int J Quantum Chem 57:501–518
6. (a) Karadakov PB, Cooper DL, Gerratt J (1998) J Am Chem Soc 120:3975–3981; (b) Blavins JJ, Karadakov PB (2001) J Org Chem 66:4285–4292
7. Schleyer PvR, Maerker C, Dransfeld A, Jiao H, van Eikema Hommes NJR (1996) J Am Chem Soc 118:6317–6318
8. (a) McWeeny R (1970) Spins in chemistry. Academic, London; (b) Eyring H, Walter J, Kimball GE (1944) Quantum chemistry. Wiley, New York
9. Deumal M, Novoa J, Bearpark M, Celani P, Olivucci M, Robb MA (1998) J Phys Chem A 102:8404–8412
10. Garavelli M, Celani P, Bernardi F, Robb MA, Olivucci M (1997) J Am Chem Soc 119:6891–6901
11. Jolibois F, Bearpark M, Klein S, Olivucci M, Robb MA (2000) J Am Chem Soc 122:5801–5810
12. Blancafort L, González D, Olivucci M, Robb MA (2002) J Am Chem Soc 124:6398–6406
13. Ismail N, Blancafort L, Olivucci M, Kohler B, Robb MA (2002) J Am Chem Soc 124:6818–6819
14. Eftink M (1991) In: Suelter CH (ed) Methods of biochemical analysis, vol 35. Protein structure determination. Wiley, New York, pp 127–203
15. Platt JR (1949) J Chem Phys 17:489
16. Pauncz R (1979) Spin eigenfunctions. Plenum, New York, p 10
17. McWeeny R (1970) Spins in chemistry. Academic, London, p 28
18. McWeeny R (1970) Spins in chemistry. Academic, London, p 37
19. Waller I, Hartree DR (1929) Proc R Soc Lond Ser A 124:119
20. Boys SF (1960) Rev Mod Phys 32:296
21. (a) Goldstein E, Beno B, Houk KN (1996) J Am Chem Soc 118:6036–6043; (b) Staroverov VN, Davidson ER (2000) J Am Chem Soc 122:7377–7385
22. Frisch MJ, Trucks GW, Schlegel HB, Gill PMW, Johnson BG, Robb MA, Cheeseman JR, Keith T, Petersson GA, Montgomery JA, Raghavachari K, Al-Laham MA, Zakrzewski VG, Ortiz JV, Foresman JB, Cioslowski J, Stefanov BB, Nanayakkara A, Challacombe M, Peng CY, Ayala PY, Chen W, Wong MW, Andrés JL, Replogle ES, Gomperts R, Martin RL, Fox DJ, Binkley JS, Defrees DJ, Baker J, Stewart JP, Head-Gordon M, González C, Pople JA (1999) Gaussian 98. Gaussian, Pittsburgh, PA
23. (a) Staroverov VN, Davidson ER (2000) J Am Chem Soc 122: 186–187; (b) Poater J, Solà M, Duran M, Fradera X (2001) J Phys Chem A 105:2052–2063; (c) Jiao H, Schleyer PvR (1998) J Phys Org Chem 11:655–662
24. Serrano-Andrés L, Roos B (1996) J Am Chem Soc 118:185–195.
25. Saito I, Sugiyama H, Yamamoto A, Muramatsu S, Matsuura T (1984) J Am Chem Soc 106:4286–4287
26. Szabo A, Ostlund NS (1996) Modern quantum chemistry. Dover, Mineola, NY, p 95
27. (a) Szabo A, Ostlund NS (1996) Modern quantum chemistry. Dover, Mineola, NY, p 253; (b) McWeeny R (1989) Methods of molecular quantum mechanics. Academic, San Diego, p 115
28. Klene M, Robb MA, Frisch MJ, Celani P (2000) J Chem Phys 113:5653–5665